35th Annual International Conference of the IEEE EMBS
Osaka, Japan, 3 - 7 July, 2013

Optical Diagnostic and Therapy Applications of Femtosecond Laser Radiation using Lens-Axicon Focusing*

Christian G. Parigger, Jacqueline A. Johnson, and Robert Splinter, *member IEEE*

Abstract— **Diagnostic modalities by means of optical and/or near infrared femtosecond radiation through biological media can in principle be adapted to therapeutic applications. Of specific interest are soft tissue diagnostics and subsequent therapy through hard tissue such as bone. Femto-second laser pulses are delivered to hydroxyapatite representing bone, and photo-acoustic spectroscopy is presented in order to identify the location of optical anomalies in an otherwise homogeneous medium. Imaging through bone is being considered for diagnostic, and potentially therapeutic, applications related to brain tumors. The use of mesomeric optics such as lens-axicon combinations is of interest to achieve the favorable distribution of focused radiation. Direct therapy by increasing local temperature to induce hyperthermia is one mode of brain tumor therapy. This can be enhanced by seeding the tumor with nanoparticles. Opto-acoustic imaging using femtosecond laser radiation is a further opportunity for diagnosis.**

I. Introduction

Application of pulsed laser radiation for photo-acoustic imaging showed significant advantages recently with both nanosecond and picosecond optical and near-infrared radiation [1]. Ultra-short laser systems that generate femto- and/or sub-pico-second pulses at rates of 80 MHz, and recently at rates 1 to two orders of magnitude higher, allows us to minimally or practically non-invasively diagnose targeted tissue volumes. Both spatially and temporally confined thermal expansion and relaxation is favorable with femtosecond laser radiation. Typical temperature rise is on the order of 1 micro-Kelvin for individual 7 nJ energy/pulse, 70 femtosecond diagnostic pulses as utilized in our studies [2, 3]. Increase in number of pulses and/or increase of average irradiation power to a few tens of milli-Watts can result in a local temperature increase on the order a few degrees Kelvin, sufficient for therapy and or interaction with nanoparticles to induce hyperthermia.

Ultrasonic waves emitted by irradiated tissue contain information about the optical as well as mechanical properties and/or abnormalities over and above thermal and mechanical characteristics. This technique reveals physiological and histological features, which provides a platform for diagnostic imaging. Ultrasonic waves can be detected with piezo-electric transducer arrays, and Radon transform techniques can be applied for forensic tomography. Femtosecond radiation is the tool for optical imaging in this work [2] together with specific focusing arrangements that include lens-axicon combinations. The temperature load in tissue [3] is also studied.

*Research supported in part by The Center for Laser Applications, The University of Tennessee Space Institute.

C. G. Parigger is with the Physics and Astronomy Department, The University of Tennessee / The University of Tennessee Space Institute, Center for Laser Applications, Tullahoma, TN 37388, USA (phone: 931-393-7338; fax: 931-393-7437; e-mail: cparigge@tennessee.edu).

J. A. Johnson is with the Mechanical, Aerospace and Biomedical Engineering Department, The University of Tennessee / The University of Tennessee Space Institute, Center for Laser Applications, Tullahoma, TN 37388, USA (e-mail: jjohnson@utsi.edu).

R. Splinter is with Valencell, Inc. 2800-154 Sumner Blvd., Raleigh, NC 27616, USA (phone: 919-747-3668; fax: 919-747-3667; e-mail: Splinter@Valencell.com).

II. Photo-acoustic Imaging

A. Energy deposition

Absorption of laser radiation causes an increase in temperature. The initial temperature rate of change and magnitude is directly related to the pulse duration, and the gradual decrease of the temperature depends on the initial irradiance distribution and thermal diffusivity. Expansion of the local medium results in a pressure pulse that emanates from focus. Laser radiation that is not absorbed will diffuse with no effect on acoustical signatures.

The energy deposition in the material will be spatially defined by the laser light distribution if thermal confinement occurs. This is satisfied when the laser pulse duration, (τ_p) is less than the thermal relaxation time (τ_r). Specifically under ultra-short (femtosecond) laser pulse irradiation, the stress relaxation is faster than the thermal relaxation as indicated by the condition:

$$\tau_p < \tau_s < \tau_r \quad . \tag{1}$$

B. Temperature and Pressure Rise

Even though the femto-second laser pulse causes a temperature rise on the same time scale, a measurable pressure variation is generated as well. The temporal (time: t) temperature profile resulting from the laser irradiation is described by the heat transfer equation as a function of location ($\vec{r}$):

$$\kappa \nabla T(\vec{r}) - \frac{\kappa}{\alpha}\frac{\partial T(\vec{r})}{\partial t} = -\beta\, T_0(\vec{r})\frac{\partial}{\partial t}H \quad . \tag{2}$$

Here, $H(x, y, z, t)$ is the absorbed electromagnetic energy density that is converted into heat per unit volume, κ represents the thermal conductivity, β the thermal expansion coefficient, and α is the thermal diffusivity. The solution to equation 2 has been studied [3,4] with a source function modeled by a Delta distribution. Subsequently, the associated pressure rise, $p\,(\vec{r}, t)$ can be calculated using material properties, such as the isothermal compressibility, γ [Pa^{-1}],

the thermal coefficient of volume expansion and β is the coefficient of thermal expansion [K^{-1}], [5],

$$\Delta p(\vec{r}) = \frac{\beta\, \Delta T(\vec{r})}{\gamma} \ . \qquad (3)$$

For example, the isothermal compressibility of hydroxyapatite can be calculated to be about 8.5×10^{-12} Pa^{-1} using a density of 3,000 kg/m^3 and a speed of sound of 6,250 m/s. A volume expansion coefficient of 20×10^{-6} K^{-1}, and a temperature rise after interaction with a 7 nJ, 70 fs laser pulse on the order of 2 μK [3], results in a pressure rate of change on the order of 5 Pa during the application of the laser pulse.

The generation of a pressure wave and its consequent propagation through the medium is governed by the non-homogeneous wave equation,

$$\nabla^2 p - \frac{1}{v^2}\frac{\partial^2}{\partial t^2} p = -\frac{\beta}{C_p}\frac{\partial}{\partial t} H \ , \qquad (4)$$

where, C_p is the specific heat at constant pressure [J/kg.K], and v is the speed of sound [cm/s] [4]. The amount of energy that is absorbed resulting from deposition of laser energy pulses depends on the optical properties of the material, specifically, on the optical absorption coefficient μ_a [cm^{-1}] and the laser energy fluence, Ψ [J/cm^2].

C. Photoacoustic Spectroscopy

The rapid absorption and associated localized temperature rise result in an acoustic resonance in response to the momentary pressure increase followed by rapid recoil of the medium under irradiation. The acoustic wave generated by the absorption of the laser radiation shows an acoustic spectrum representative of the energy absorbed and the respective dimensions of the constituents in the interaction volume. As the acoustic spectrum migrates radially outward through inhomogeneous tissue, the spectral profile will be affected by acoustic filtering in the direction of observation. Additional boundary conditions and the diversity of material properties in the laser-tissue interaction volume will result in a mixture of discrete and continuous spectral bands of acoustic frequencies. These frequencies contain information about the microscopic scale elements responsible for the respective spectra. Measurement results and analysis by use of Fourier transform techniques is further elaborated in Section IV. B.

D. Advantages of Femtosecond Laser Radiation and Femtosecond Spectroscopy

The advantages of femto-second laser pulses for precise material processing is due to that fact that the interaction of the ultra-short laser pulses with the target material is thermally confined [6, 7], creating negligible thermal and mechanical damage to the surrounding area during laser imaging. The temperature profile can be modulated temporally and spatially which is beneficial for photo-acoustic imaging. Particularly in sensing and precise treatment options, diminished pressure amplitudes are important, otherwise cracks several tens of microns in size would be generated, thus weakening the structural integrity.

III. Materials and Methods

Laser light was delivered in femto- second mode in 40 ms trains of femtosecond laser pulses at a rate of 76 MHz using a Spectra Physics Tsunami Ti:Sapphire laser, operating at 820 nm with 7nJ energy per pulse and 70 fs pulse-width. The investigations were performed on a hard tissue configuration constructed from hydroxyapatite [8-9]. Various methods were utilized for characterization and measurement of femto-second radiation [10-12].

The hydroxyapatite sample was used in a cubical configuration that allowed us to conveniently place the acoustic sensor placement as well as well-defined boundary conditions for numerical analysis. Material insertions at various depths were representative of optically and mechanically well-defined soft-tissues. Optical perturbations were introduced in predetermined locations within the solid medium. The medium was composed of various fixed diameter particle-aggregates, which scattered and had selective absorption characteristics representative of specific biological phenomena and features.

For characterization of the irradiance distribution, an experimental study utilizes a lens-axicon doublet for beam shaping both in diagnostic and therapy mode [13-14]. For the experiments, a He-Ne laser radiation was used; however, recent work confirms focusing modeling and characteristics [14] also apply to femtosecond laser radiation [15]. Figure 1 shows the experimental arrangement.

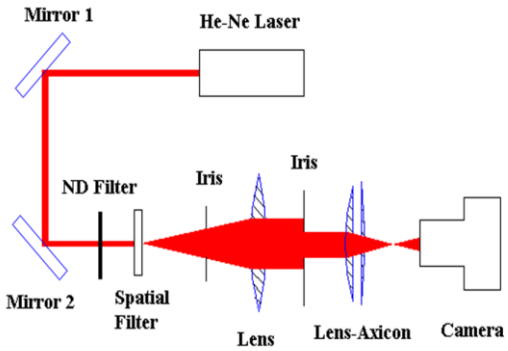

Figure 1: Experimental arrangement for accurate measurements of focal irradiance distributions from lens-axicon doublets.

IV. Results

A. Lens-Axicon Light Delivery

Measurement of the focal distribution is accomplished by systematically moving the lens-axicon doublet and recording images at the different positions. The expected lens-axicon distribution, for a converging axicon is composed of a focal line, followed by a focal ring. The qualitative behavior is illustrated in a combined image obtained by moving a reflecting card while illuminating the card with a strobe light. Figure 2 illustrates the results.

Conversely, a diverging lens-axicon doublet shows formation of a focal ring followed by a focal line. The qualitative behavior of a diverging lens-axicon doublet can be studied with a pulsed Nd:YAG laser (22 ns pulse width,

23 mJ energy/pulse) and burn-paper. Figure 3 shows formation of the focal ring, as indicated by the arrow in the second set near focus of the lens.

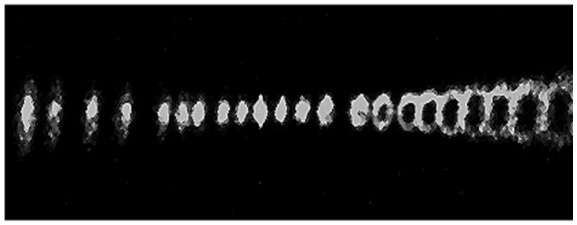

Figure 2: Qualitative converging lens-axicon focusing characteristics.

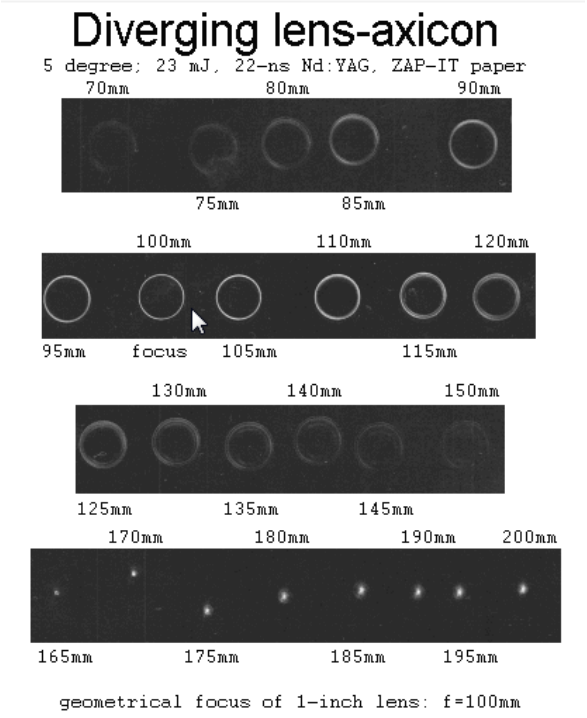

Figure 3: Qualitative behavior of diverging lens-axicon doublet.

The radius, R_o , of the focal ring can be calculated [14] from

$$R_o = (n_{Axicon} - 1)\,\alpha_{Axicon}\,f \qquad (5)$$

Here, f is the focal length of the lens, α_{Axicon} and n_{Axicon} are the apex angle and refractive index of the axicon, respectively. For some physiological applications, generation of a focal ring structure, followed by a line focus may be preferred.

Detailed studies of the line and ring structure are further reported to address qualitative and quantitative agreements. We present results specifically for the focal line characteristics of a converging lens-axicon. The theory predictions of focusing characteristics [14] agree nicely with experimental results. While the overall structure of focusing characteristics can be predicted with geometric optics, i.e., focal line structure and focal ring structure, the detailed predictions require the solution of diffraction integrals. Figures 4 - 5 display experimental and matching theoretical irradiance maps, respectively. We prefer a base 10 logarithm pseudo-color scale to illustrate the results obtained with a 256 grey-level (8-bit) camera.

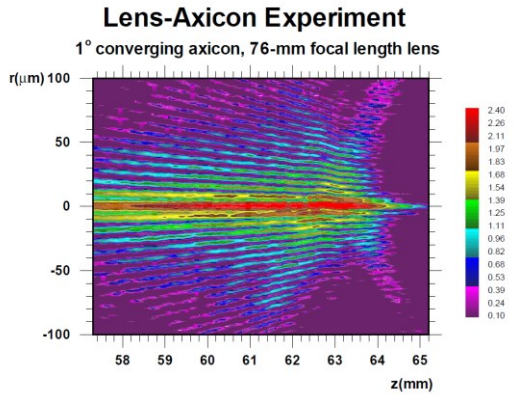

Figure 4: Experimentally recorded characteristics in Lens Axicon focus.

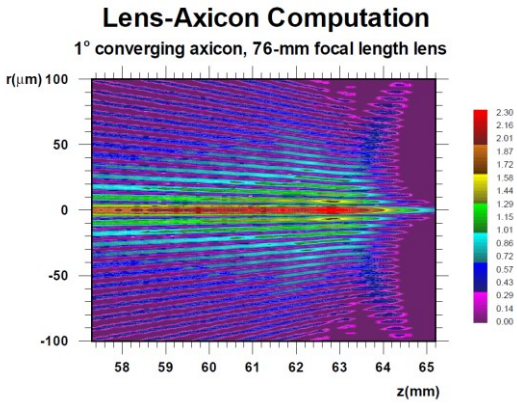

Figure 5: Computational results from evaluation of diffraction integrals show good qualitative and quantitative agreement.

The lens-axicon light delivery provides the ideal vehicle for targeted light delivery into a highly scattering medium with minimized distortions resulting from dispersion and scattering. This can result in a sharp reduction for the radiance requirements of the probing source with inherent lower risks for thermal and mechanical damage.

B. PhotoAcoustic Sensing

Scattering, absorption and acoustic spectral distribution experiments [2-4, 8-12] with 70 fs laser pulses indicate promise for light penetrating a phantom of hydroxyapatite resembling hard tissues found in human anatomy. Figure 6 illustrates the recorded photo-acoustic spectrum.

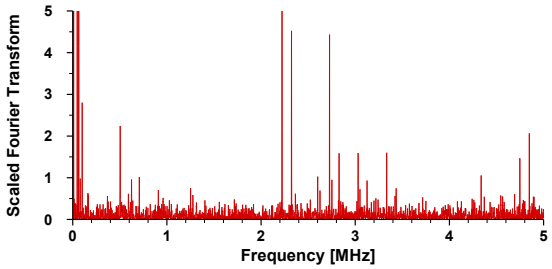

Figure 6: Fourier transform of the signal from a hydroxyapatite cube with Intralipid scattering and attenuating solution in a preformed canal at 2 mm from the surface.

In the preliminary measurements [8], acoustic signatures were recorded with respect to a hydroxyapatite phantom for which localized perturbations were made with scattering and absorbing constituents. An acoustical point source was utilized near the phantom, and we studied the emanating acoustical signals.

V. Discussion

Lens-Axicon focusing has been proposed to achieve a tightly focused acoustic source spot at a predetermined location in the inhomogeneous tissue model [13]. Additionally, by increasing the energy/pulse, diagnostics can be turned into a therapeutic mode including specific focusing designs to induce hyperthermia and necrosis of brain tumors [13]. The size of cancer cells has been found to be larger in certain cancer tissue cells compared to the normal cell-line of representative tissues under investigation [16-19]. The dimensions of the cell nucleus carry an acoustic signature that can be analyzed with spectral signal processing for diagnostic value in cancer detection and localization. Reconstruction of the acquired signals from multiple locations will generate a tomographic image using techniques such as Radon transform, to reveal microscopic details [20].

Femto-second laser radiation shows several advantages over other radiation therapy [21], in part due to precise control of spatial and temporal beam-shapes that is expected to allow us to focus on specific areas of interest for radiation dose. Augmentation of femto-second imaging and therapy can be accomplished with nano-particles including, e.g., hybrid iron/gold nano-particles [22-24]. Most importantly, the application of Bessel beams, or the use of lens-axicon doublets, is expected to be favorable for interaction of short-pulse radiation with tissue. Future studies are required to show thermal loads [3] from individual and/or repetitive or therapeutic short-pulsed laser radiation, and to explore sustenance of intensity distributions [14] in tissue prior to therapeutic application through hard tissue [21].

VI. Conclusion

The use of photo-acoustic imaging as well as coherent imaging and ultra-short optical pulse spectroscopy show promise for evolution into commercial sensing devices with the likelihood of procurement of detailed tissue information. With continuously growing numbers of imaging devices there is still a gap between the clinical demand for detail and the capabilities of delivering these in a timely fashion, safely, and at a reasonable cost.

Acknowledgment

We thank Dr. Pavlina J. Pike (maiden name: Dr. Pavlina J. Jeleva) and Dr. Guoming Guan for their interest, and acknowledge support in part by The University of Tennessee Space Institute, Center for Laser Applications.

References

[1] L.V. Wang, *Photoacoustic Imaging and Spectroscopy* (Taylor &Francis, 2009).

[2] P. Pike, C. Parigger, and R. Splinter, "High Resolution Biological Imaging Techniques," in Laser Pulse Phenomena and Applications, F. J. Durante, Ed. Rijeka, Croatia, Intech, 2010, pp. 433-458.

[3] P. Pike, C. Parigger, R. Splinter, and P. Lockhart, "Temperature distribution in dental tissue after interaction with femtosecond laser pulses," Appl. Opt. 46, pp. 8374-8378, 2007.

[4] C.G. Parigger, J.A. Johnson, and R. Splinter, "Physiological sensing through tissue with femto-second laser radiation," 9th International Conference of High-Capacity Optical Networks & Emerging/Enabling Technologies, Dec 12 -14, Istanbul, Turkey, 2012.

[5] A.L. McKenzie, "Physics of thermal processes in laser-tissue interaction," Phys. Med. Biol. 35, pp. 1175-1209, 1990.

[6] B.N. Chichkov, C. Momma, S. Nolte, F. von Alvensleben, A. Tünnermann, "Femtosecond, picosecond and nanosecond laser ablation of solids," Appl. Phys. A 63, pp.109-115, 1996.

[7] J. Serbin, T. Bauer, C. Fallnich, A. Kasenbacher, and W.H. Arnold, "Femtosecond lasers as novel tool in dental surgery," Appl. Surf. Sci. 197-198, 2002, pp. 737-740.

[8] P. Pike, "Photo-acoustic analysis of dental materials and tissue," Ph.D. dissertation, Dept. Phys. Astron., The University of Tennessee, Knoxville, Tennessee, 2005.

[9] J. Mukherjee, and S. Chakraboty, "Modeling of temperature distribution within a dental profile on account of laser irradiation," Int. J. Biom. Eng. Techn. 3, pp. 186-198, 2010.

[10] X. Gu, S. Akturk, A.Shreenath, Q. Cao, and R. Trebino, "The measurement of ultrashort light – simple devices, complex pulses,"in: Femtosecond Laser Spectroscopy, P. Hannaford, Ed. New York, Springer, 2005, pp. 61-86.

[11] P. O'Shea, M. Kimmel, X. Gu, R. Trebino, "Highly simplified device for ultrashort-pulse measurement," Opt. Lett. 26, pp. 932-934, 2001.

[12] G. Guan, "On the analysis of emission spectra and interference images," Ph.D. dissertation, Dept. Phys. Astron., The University of Tennessee, Knoxville, Tennessee, 1999.

[13] C. G. Parigger, J. A. Johnson, and R. Splinter, "Medical Diagnostic And Surgery Using Laser Radiation With Lens-Axicon Focusing," UT Research Foundation, Knoxville, TN, 2012, patent pending.

[14] C. Parigger, Y. Tang, D.H. Plemmons, and J.W.L. Lewis, "Spherical aberration effects in lens–axicon doublets: theoretical study," Appl Opt. 36, pp. 8214-8221 (1997).

[15] T. Anderson, C. Zuhlke, J. Brice III, D. Alexander and C.G.Parigger, "Evidence of Near Field Filaments and Focusing Effects on Femtosecond LIBS," NASLIBS Conf. Proc., Clearwater, FL, 2011.

[16] X. Wang, Functional Photoacoustic Tomography of Animal Brains, PhD Thesis, Texas A&M University 2004.

[17] X. Xie, Tumor Angiogenesis O-saturation, Glucose and Amino-Acid Metabolisms Study using Functional Imaging, PhD Thesis, Texas A&M University 2008.

[18] X. Wang, Y. Pang, G. Ku, X. Xie, G. Stoica, L.V. Wang, Noninvasive laser-induced photoacoustic tomography for structural and functional in vivo imaging of the brain, Nat Biotechnol. 2003 21(7): 803-806.

[19] W.J. Brown, J.W. Pyhtila, N.G. Terry, K.J. Chalut, T.A. D'Amico, T.A. Sporn, J.V. Obando, and A. Wax, Review and Recent Development of Angle-Resolved Low-Coherence Interferometry for Detection of Precancerous Cells in Human Esophageal Epithelium, IEEE J. Sel. Topics Quant. Electr.14(1), 2008, 88-97.

[20] L.V. Wang, Photoacoustic tomography: ultrasonically breaking through the optical diffusion limit, SPIE proceedings Photonics Europe 2012.

[21] R. Meesat, H. Belmouaddinea, J-F Allarda, C. Tanguay-Renauda, R. Lemaya, T. Brastaviceanua, L. Tremblaya, B. Paquettea, J. Richard Wagnera, J-P Jay-Gerina, M. Lepagea, M.A. Huelsa, and D. Houdea, Cancer radiotherapy based on femtosecond IR laser-beam filamentation yielding ultra-high dose rates and zero entrance dose, PNAS 2012 109 (38) E2508-E2513.

[22] A.Oraevsky, Gold and silver nanoparticles as contrast agents for Optoacoustic Tomography, Tomography, in: Photoacoustic Imaging and Spectroscopy (Ed. L. V. Wang), (Taylor &Francis 2009) chapter 30 pp 373-386.

[23] S. Emelianov, S. Mallidi, and T. Larson, Photacoustic Imaging and Therapy Utilizing Molecular Specific Plasmonic Nanoparticles, in: Photoacoustic Imaging and Spectroscopy (Ed. L. V. Wang), (Taylor &Francis 2009) chapter 32 pp 399-407.

[24] M-R Choi, R. Bardhan, K.J. Stanton-Maxey, S. Badve, H. Nakashatri, K.M. Stantz, N. Cao, N.J. Halas, S.E. Clare, "Delivery of nanoparticles to brain metastases of breast cancer using a cellular Trojan horse", Cancer Nanotechnology 3, pp. 47-54, 2012.